J MATER SCI **41** (2006) 2667–2671

Formation of iron silicide nano-islands on Si substrates by metal organic chemical vapor deposition under electron beams

M. TANAKA*, F. CHU
High Voltage Electron Microscopy Station, National Institute for Materials Science, 3-13, Sakura, Tsukuba, 305-0003, Japan
E-mail: tanaka.miyoko@nims.go.jp

M. SHIMOJO
High Voltage Electron Microscopy Station, National Institute for Materials Science, 3-13, Sakura, Tsukuba, 305-0003, Japan; Precision and Intelligence Laboratory, Tokyo Institute of Technology, 4259 Nagatsuta-cho, Midori-ku, Yokohama, 226-8503, Japan

M. TAKEGUCHI, K. MITSUISHI, K. FURUYA
High Voltage Electron Microscopy Station, National Institute for Materials Science, 3-13, Sakura, Tsukuba, 305-0003, Japan

Published online: 17 April 2006

Electron-beam induced chemical vapor deposition (EBI-CVD) of $Fe(CO)_5$ was performed on both Si (111) and (110) substrates at 673–873 K inside an ultrahigh vacuum transmission electron microscope. The formation of iron silicide islands was observed on both substrates. Cubic silicide nano-rods were formed on Si(111) substrates by EBI-CVD with focused electron beams. The formation of β-$FeSi_2$ islands was mainly observed on Si(110) substrates by EBI-CVD when the electron beam was broadly spread. It was shown that the size and the intensity of the electron beam played a significant role in EBI-CVD and affected the CVD process extensively.

1. Introduction

Recently, there has been considerable interest in studying the first stage of the layer growth by chemical vapor deposition (CVD) because the subsequent film growth depends heavily on this atomistic process. The early stages of laser-induced chemical vapor deposition have been investigated extensively and many fundamental aspects of surface photochemistry have been explained [1, 2]. However, very little experimental work has been performed to elucidate the initial stages of thermal, plasma-enhanced, or beam-assisted CVD. Scanning tunneling microscopy (STM) is beginning to play an important role in clarifying layer morphology during the early stages of metal deposition of thermal CVD [3–5].

Deposition of transition metals by CVD is of significant importance because of their wide applicability and for the potential applications of their silicides. At the same time, these metals are relatively easy to deposit from carbonyls and fluorides with high vapor pressures at room temperature. $Fe(CO)_5$ is one of these metal-organic precursors, for which the dissociation reaction is known to be relatively clean. Kunz *et al*. reported the formation of iron films on Si substrates by low-energy electron-beam assisted CVD at elevated temperatures without any detectable carbon from Auger spectroscopy [6]. The early stages of Fe deposition via pyrolysis of $Fe(CO)_5$ onto clean Si(001) substrates were investigated using STM [3]. Moreover, iron silicide layers of good quality have been obtained with this precursor. Thibaudau *et al*. observed the formation of thin cubic-$FeSi_2$ islands with triangular shapes on Si(111)-7 × 7 surfaces via CVD by STM [4]. Even much thicker epitaxial β-$FeSi_2$ films of high quality have been prepared successfully by low pressure CVD [7].

*Author to whom all correspondence should be addressed.
0022-2461
DOI: 10.1007/s10853-006-7868-x

In this article, we present a study of Fe deposition on Si substrates at elevated temperatures by electron-beam induced CVD (EBI-CVD). EBI-CVD is a unique nanofabrication method which has an advantage over others of allowing direct fabrication with geometrical flexibility. Nanostructures of the materials of less than 5 nm have been fabricated successfully with nm-sized probes by EBI-CVD [8, 9]. In the present study, the formation of very thin iron silicide islands from $Fe(CO)_5$ precursor gas is investigated on both Si(111) plan-view substrates and Si(110) profile-view substrates under electron beams. The effect of the electron beams on the formation of silicide will be discussed.

2. Experiment

All the experiments were done in a UHV-TEM (JEM-2000VF) with an accelerating voltage of 200 kV and with a base pressure of less than 5×10^{-8} Pa. Rectangular Si(111) and Si(110) specimens ($2 \times 7 \times 0.2$ mm) were thinned into TEM specimens by mechanical dimpling and chemical etching ($HF:HNO_3 = 1:9$). They were chemically cleaned and were resistively heated in a pre-treatment chamber of the microscope at 900 K for one night and at 1300 K for several hours until the thinnest part became contamination-free. The surface cleanness was confirmed by observing the diffraction pattern of the 7×7 superstructure in either plan view or profile view mode after cooling down the specimens to room temperature.

A gas inlet system with a variable leak valve is attached to the microscope column and supplies metal-organic gases directly into the sample stage. The details of this system are described elsewhere [9]. The precursor gas was $Fe(CO)_5$. Pressure during deposition was set at 2×10^{-6} Pa, and the substrate temperatures were varied between 673 K and 873 K. The beam intensity during the plan-view and profile-view deposition were about 5×10^3 –5×10^4 A/cm^2 and 10–10^2 A/cm^2, and the beam sizes were about 1 nm in diameter and 200 nm, respectively. TEM observation was done after the vacuum recovered to the background pressure level in order to avoid incidental deposition.

3. Results and discussion

3.1. Plan-view observation

Focused electron beams were irradiated on Si(111) plan-view substrates in the presence of the precursor. As a result, nano-rod-shaped islands were grown regardless of the substrate temperature. The islands started to grow from the point of incidence of the electron beams, and their typical images are shown in Fig. 1. The irradiation time for each rod was 5 s. Electron-energy loss spectroscopy of the rods revealed that they contained only Si and Fe. At this temperature range of 673–873 K, it is not expected

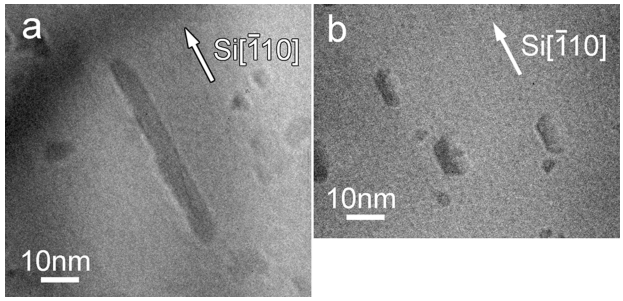

Figure 1 TEM micrographs of iron silicide nano-rods grown on a Si(111) substrate. (a) A nano-rod of high aspect ratio, and (b) nano-hexagons. Both types of rods grow parallel to the Si[$\bar{1}$10] direction.

that $Fe(CO)_5$ molecules adsorb on the surface. The deposits are produced by electron-beam ligand scission of molecules close to the surface or thermal decomposition of molecules into more unstable subcarbonyls that easily lose the remaining ligands at temperatures above 398 K [10]. Thus Fe atoms are deposited at close to the molecular decay sites initiated by electron-beam irradiation. The nano-rods must be formed at those possible adsorption sites near these decay sites, which could be grain boundaries, antiphase lines of the 7×7 domains, steps as indicated before [4], or the defects formed by electron-beam irradiation. After nucleation, the continuous supply of Fe atoms promoted the nuclei to grow further along the long axis directions of the rods.

Their shapes varied from long nano-rods of high aspect ratio as shown in Fig. 1a to short nano-rods of low aspect ratio (more like hexagons) as shown in Fig. 1b. In either case, their preferential growth direction was one of the three equivalent Si⟨110⟩. The difference in their shapes reflected the orientation of the substrate surface as we reported before [11]. When the surface is a flat terrace and its orientation is flat-on Si(111) plane, the islands tend to grow into hexagons or truncated triangles. When it is faceted and is inclined toward one of the Si⟨111⟩ directions, they grow in the perpendicular direction (Si⟨110⟩). The substrate surface normal was determined from that spot splitting of corresponding diffraction pattern which occurs parallel to the direction of the incline. On the inclined surfaces, there exists anisotropy of the substrate lattice along the horizontal direction (in the present case, Si⟨110⟩) and the inclination direction (normal to Si⟨110⟩). The horizontal growth is energetically favorable due to the small lattice mismatch. However, along the inclination direction, bond stretching, compression, or bond-angle deformation of the atoms at the interface must occur during growth, which restricts the growth along that direction severely.

High-resolution images of the islands and the corresponding diffraction pattern (Fig. 2) show images and patterns almost identical to those of Si(111) [11]. This implies that the island phase is cubic iron silicide of almost the same planer distances as those of Si. Besides

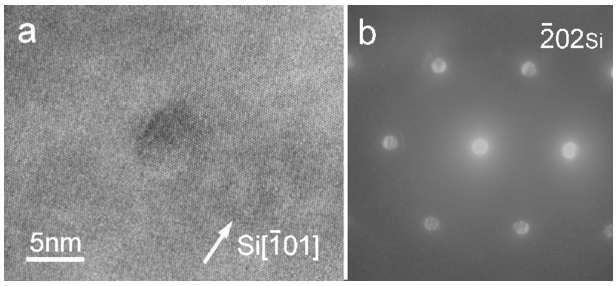

Figure 2 (a) High-resolution image of one of the nano-rods of low aspect ratio, and (b) corresponding diffraction pattern. The nano-rods has a cubic structure.

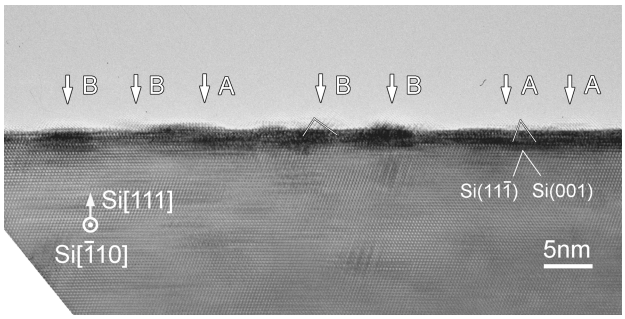

Figure 3 A TEM micrograph of iron silicide islands grown on a Si(111) edge plane at about 700 K. While islands A retain the plane spacings and plane angles of the Si substrates, islands B seems to have different structure.

several equilibrium silicide phases, there are two types of cubic iron silicides that are metastable in thin-film form; either an $FeSi_{1+x}$ ($x = 0-1$) phase having a CsCl structure and belonging to the primitive cubic Bravais lattice with a lattice parameter close to half of the Si lattice constant [12], or γ-$FeSi_2$ phase having a fluorite structure CaF_2 and belonging to a face-centered cubic Bravais lattice with a lattice parameter almost equal to the Si[13]. The (111) planes of both phases grow epitaxially on Si(111) with almost perfect lattice match. Looking from the Si[111] azimuth, their diffraction spots ($FeSi_{1+x}$ 110 or γ-$FeSi_2$ 220) almost overlap with that of Si 220. Thus it is impossible to distinguish from plan view imaging which is the exact phase grown here.

3.2. Profile-view observation

In the case of EBI-CVD on Si(110) profile-view substrates, focused-electron beam irradiation caused sputtering of the substrates because the region of interest is the interface between the surface layer and the vacuum. Thus broader electron beams were used for irradiation and the deposition time was more than 10 min.

When the substrate temperature was about 673–723 K, formation of ultra-thin islands was observed on Si(111) edge planes as shown in Fig. 3. The islands are indicated by arrows. The typical height of the islands was about 3–5 monolayers (ML), so it was impossible to identify their structure unambiguously. However, some of the islands seem to maintain the plane spacings and plane angles of Si(111) and Si(001) of the substrate (labeled A in the figure) and are therefore assumed to have a cubic structure. On the other hand, other islands (labeled B) seemed to have a different structure. This structure is most likely to be β-$FeSi_2$ type, which will be discussed in more detail below. Anyhow, the islands were too thin and too small to determine their structures unambiguously. Type A islands tend to appear as flatter and shorter islands.

When the substrate temperature was about 773 $\pm$ 25 K, the islands became taller (3–10 ML). All of them seemed to have type B structure, although sometimes it was difficult to identify their structure due to the thinness of the islands.

When the substrate temperature was about 823–873 K, the islands became taller (more than 10 ML) and larger, and all of them were identified as β-$FeSi_2$ which has a base-centered orthorhombic structure with $a = 0.9863$ nm, $b = 0.7791$ nm, and $c = 0.7833$ nm. This phase is very stable as thin films. Fig. 4 shows the islands grown on substrates of different orientations. In Fig. 4a, the islands were grown on Si(111) edge plane. Some parts of the surface are vicinal to Si(111). It is recognized that all the islands have an epitaxial relationship of either $(110)_\beta//(111)_{Si}$ with $[001]_\beta//[110]_{Si}$, or $(101)_\beta//(111)_{Si}$ with $[010]_\beta//[110]_{Si}$ (type I), which is determined from diffraction pattern in Fig. 4b. These two relationships are almost indistinguishable due to the small difference between b and c. The islands are under compressive strain of 2.0 (or 1.4)% and tensile strain of 5.5 (or 5.3)% in the c (or b) and diagonal of a and b (or c) directions, respectively. Islands on the Si(001) plane maintain the same planar relationship (Fig. 4c), although another relationship of $(100)_\beta//(001)_{Si}$ with $[001]_\beta//[110]_{Si}$ is also observed (type II). Again an alternative relationship of $(100)_\beta//(001)_{Si}$ with $[010]_\beta//[110]_{Si}$ is possible. In the corresponding diffraction pattern (Fig. 4d), diffraction spots of type I relationship are indicated by solid lines and those of type II by dashed lines. The type I relationship has the lowest interfacial energy with the Si(111) interface. Thus the islands prefer to grow into the substrate and have Si{111} facets matching with β-$FeSi_2$ {220} planes as can be observed in the figure from the moiré fringes (indicated by an arrow with 'M'). These moiré fringes arise from the interference between the (440) β-$FeSi_2$ and the (111) Si reflections. On the other hand, type II islands are less strained with a Si (001) interface. The misfit is about $+1.4$% and $+2.0$%, in b and c directions, respectively, if we can apply bulk data here. Thus the islands do not grow into the substrate as the type I islands do.

3.3. Effect of the electron beam on CVD

In the early stages of conventional CVD of $Fe(CO)_5$ precursor at elevated temperature, the molecules almost

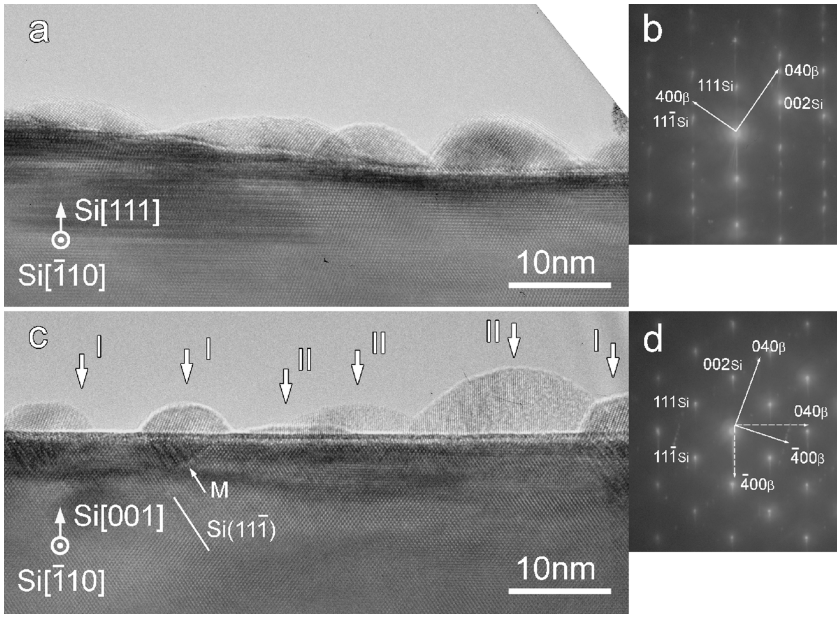

Figure 4 TEM micrographs and corresponding diffraction patterns of iron silicide islands grown at about 850 K. (a) Islands grown on a Si(111) edge, (b) its diffraction pattern showing type I epitaxial relationship, (c) islands grown on a Si(001) edge with two types of epitaxial relationships, and (d) its diffraction pattern showing type I (solid lines) and type II (dashed lines) relationships. Moiré fringes in (c) implies the growth of islands into the Si substrate.

simultaneously react on dissociative adsorption sites (strong nucleophilic sites), deposit as Fe clusters, and form iron silicide islands [4]. At relatively low temperature, Fe clusters formed by CVD tend to grow bigger than clusters formed by typical Fe evaporation due to the autocatalytic effect, in which previously deposited Fe atoms activate decomposition of both partially coordinated $Fe(CO)_x$ and $Fe(CO)_5$ molecules incident on the surface through ligand exchange [3, 10]. At the high temperatures used here, this may not play an important role and Fe accumulation may not occur on the substrate surface. It has been reported that epitactic growth of $FeSi_2$ takes place in the phase sequence of cubic, α, and β with increasing Fe concentration [14]. Itakura *et al*. also reported that the lower temperature and the higher Fe concentration suppress the formation of α-$FeSi_2$ and promote the formation of β-$FeSi_2$ [15]. Thus in the case of conventional CVD, fewer Fe atoms concentrate on the surface and formation of cubic iron silicide is observed. On the other hand, broad beam EBI-CVD drastically promotes dissociation of $Fe(CO)_5$ molecules [6]. This does not happen only at the dissociation sites but in the area where electron beams are irradiated above and on the surface. The dissociated Fe atoms diffuse to the nucleation sites (presumably to the dissociative adsorption sites) to contribute to the further growth of the silicide islands. All this implies a higher concentration of Fe atoms on the surface than during conventional CVD cases and hence formation of β-$FeSi_2$ islands, as frequently observed in the present profile-view study.

To compare with the broad-beam experiments previously described, focused-beam EBI-CVD was performed using a small amount of precursor gas in a much more localized area. The amount of exposure is less than 0.1 langmuir ($1L = 133 \times 10^{-8}$ Pa sec) for each rod, and the area where the dissociation occurred can be approximated as a column of 1 nm in diameter and of several nm in height at most. This may not be enough to cause excess Fe concentration, and results in the formation of cubic iron silicide rods rather than β-$FeSi_2$ rods.

The present results suggest that broad beam EBI-CVD could be used to promote certain kinds of chemical reaction which are not easy to induce by conventional CVD. At the same time focused beam EBI-CVD is quite effective in provoking desired reaction at a desired position.

4. Conclusion

In conclusion, we have observed the development of silicide island morphology and structure during EBI-CVD of $Fe(CO)_5$ on Si substrates at 673–873 K in both plan-view and profile view TEM. Nano-rods of different aspect ratio were formed by focused beam EBI-CVD on plan-view Si(111) substrates. The nano-rods had the structure of cubic iron silicide. Formation of β-$FeSi_2$ islands were mainly observed on profile-view Si(110) substrates by broad beam EBI-CVD. It was suggested that broad-beam EBI-CVD assisted dissociation of precursor to contribute to accumulation of Fe atoms on the substrate, while focused-beam EBI-CVD induced a local reaction in a position-controlled manner.

References

1. J. R. SWANSON, C. M. FRIEND and Y. J. CHABAL, *J. Chem. Phys.* **87** (1987) 5028.
2. N. S. GLUCK, Z. YING, C. E. BARTOSCH, and W. HO, *ibid.* **86** (1987) 4957.

3. D. P. ADAMS, L. L. TEDDER, T. M. MAYER, B. S. SWARTZENTRUBER and E. CHASON, *Phys. Rev. Lett.* **74** (1995) 5088.
4. F. THIBAUDAU, L. MASSON, A. CHEMAM, J. R. ROCHE and F. SALVAN, *J. Vac. Sci. Technol.* **A 16** (1998) 2967.
5. M. KNEPPE, V. DORNA, P. KOHSTALL, E. KOT and U. KÖHLER, *Surf. Sci.* **454–456** (2000) 802.
6. R. R. KUNZ and T. M. MAYER, *J. Vac. Sci. Technol.* **B 6** (1988) 1557.
7. K. AKIYAMA, S. OHYA, H. TAKANO, N. KIEDA and H. FUNAKUBO, *Jpn. J. Appl. Phys.* **40** (2001) L460.
8. K. MITSUISHI, M. SHIMOJO, M. HAN and K. FURUYA, *Appl. Phys. Lett.* **83** (2003) 2064.
9. M. TANAKA, M. SHIMOJO, K. MITSUISHI and K. FURUYA, *Appl. Phys.* **A 78** (2004) 543.
10. R. R. KUNZ and T. M. MAYER, *Appl. Phys. Lett.* **50** (1987) 962.
11. M. TANAKA, F. CHU, M. SHIMOJO, M. TAKEGUCHI, K. MITSUISHI and K. FURUYA, *ibid.* **86** (2005) 183104.
12. N. E. CHRISTENSEN, *Phys. Rev.* **B 42** (1990) 7148.
13. H. VON KÄNEL, K. A. MÄDER, E. MÜLLER, N. ONDA and H. SIRRINGHAUS, *ibid.* **B 45** (1992) 13807.
14. M. BEHAR, H. BERNAS, J. DESIMONI, X. W. LIN and R. L. MALTEZ, *J. Appl. Phys.* **79** (1996) 752.
15. M. ITAKURA, D. NORIZUMI, T. OHTA, Y. TOMOKIYO and N. KUWANO, *Thin Solid Films* **461** (2004) 120.